Thermoremanence acquisition and demagnetization for titanomagnetite under lithospheric pressures

Nicolas Launay, Pierre Rochette, Yoann Quesnel, François Demory, Natalia S. Bezaeva, Dominique Lattard

Thermoremanence acquisition and demagnetization for titanomagnetite under lithospheric pressures.

Nicolas Launay[1], Pierre Rochette[1], Yoann Quesnel[1], François Demory[1], Natalia S. Bezaeva[2, 3] and Dominique Lattard[4]

[1]Aix-Marseille Université, CNRS, IRD, UM34, Aix-en-Provence, France

[2]Institute of Physics and Technology, Ural Federal University, Ekaterinburg, Russia

[3]Institute of Geology and Petroleum Technologies, Kazan Federal University, Kazan, Russia

[4]Institute of Earth Sciences, Heidelberg University, Heidelberg, Germany

Key Points:

- Titanomagnetite unblocking temperature increases with pressure at a rate of 10-20 K/GPa.
- Thermoremanent magnetization acquired under pressure higher than 400-600 MPa is twice as strong as TRM acquired at atmospheric pressure.
- Results suggest that the magnetized part of the lithosphere is thicker than currently considered, and that 50 to 60% of its magnetization may be underestimated.

Abstract

The geological sources of large-scale lithospheric magnetic field anomalies are poorly constrained. Understanding the magnetic behavior of rocks and minerals under the pressures and temperatures encountered at large crustal depths is particularly important in that task. The impact of lithospheric pressure is not well known and most of the time neglected in numerical models of the geological sources of magnetic anomalies. We present thermal remanent magnetization (TRM) acquisition, and stepwise thermal demagnetization on synthetic titanomagnetite dispersed powder, within an amagnetic cell under hydrostatic pressure up to 1 GPa. TRM is measured after thermal cycling within a cryogenic magnetometer. Pressure-dependent increase in the Curie temperature (initially in the 50-70°C range) is observed, mostly between 0.3 and 0.6 GPa, on the order of 20 K/GPa. TRM intensity also increases with pressure up to 200% at 675 MPa, although the pressure variation with temperature inside the cell complicates the interpretation.

1 Introduction

The Earth's lithosphere magnetization is governed by the different magnetic properties of its constituent rocks and by the pressure and temperature (P**,** **T**) conditions. The geological sources of large-scale lithospheric magnetic field anomalies are poorly constrained, even if satellite and airborne measurements of Earth magnetic field show that they should lie partly or mostly in the deep crust *[Langel and Hinze, 1998; Vervelidou et al., 2015]*. Data from the current ESA SWARM satellite mission help to better characterize small-scale features of the lithospheric magnetic field *[Thébault et al., 2016],* but we are still missing good models concerning the deepest (and somehow long-wavelength) possible magnetization. Indeed, the characterization of these sources from magnetic field data needs forward and inverse numerical modeling, which cannot provide unique solutions. A recent example concerns the expected magnetization of the upper mantle in some geodynamic context [*Ferré et al., 2014; Friedman et al., 2014*] which should be taken into account in the source numerical models constrained by satellite data. Therefore, understanding the magnetization of rocks at large crustal depths becomes fundamental for constraining the nature and characteristics of magnetic sources in the models.

While the effect of high temperatures on the magnetic properties of minerals has been well known for half a century *[Dunlop et al., 1997]*, the impact of pressure is still unclear *[Samara et Giardini, 1969]*, in particular regarding thermoremanence (TRM) acquisition.

Pressure-induced changes in the properties of magnetic minerals at room temperature (RT: 293 K or 20°C) have been rather extensively studied. Anvil-type apparatuses with solid confinement of the samples are commonly used in such studies, allowing pressure up to several GPa *[Gilder et al., 2008]*. Unfortunately, such an apparatus generates significant deviatoric stresses which do not reproduce the condition of natural hydrostatic pressure in the deep lithosphere. Furthermore, deviatoric plastic strain affects irreversibly the magnetic properties of the sample. To avoid this issue, hydrostatic pressure transmitted in a pressure cell via a liquid medium may be used *[Demory, et al., 2013]*. Such solution, used here, limits the maximum pressure available to 2 GPa (~70 km depth) which is relevant for lithospheric magnetization models.

Concerning remanence the demagnetizing effect of hydrostatic pressure, even though lesser than the one generated by deviatoric stress, has been emphasized for terrestrial and extraterrestrial minerals and rocks *[Pearce et al., 1981; Bezaeva et al., 2010]*. Isothermal remanence (IRM) acquisition under pressure has shown that both IRM intensity and coercivity can significantly increase under pressure, *[Gilder, et al., 2004; Gilder, et al., 2008; Demory, et al., 2013]*. Magnetic measurements under variable temperature in the GPa pressure range are rare. *Schult* [*1970*] determined the Curie point of titanomagnetite at pressures up to 6 GPa, revealing an increase between 10 and 18 K/GPa depending on titanium content (see also *Samara and Giardini, [1969]* for pure magnetite). Recently, by cycling our pressure cell from 240 to 293 K, we have shown that the hematite Morin transition temperature increases linearly with pressure up to 1.6 GPa at a rate of 25 K/GPa [*Bezaeva, et al., 2015*].

Though some of these results were primarily gathered in order to understand the effect of meteor impacts on the magnetism of shocked rocks, they can also be applied to the magnetization of deep crustal rocks. The purpose of the present contribution is to provide a study focused on thermal magnetization and demagnetization of magnetic minerals under deep lithospheric pressures.

2 Samples and Methods

TRM acquisition and demagnetization under pressure were measured on synthetic titanomagnetites with Curie point values close to RT, because our pressure cell works best at temperatures slightly above RT.

Two samples, described in detail by [*Engelmann et al., 2010*], were selected: F57 x 3 and 6F72 x 4.4, hereafter named LS57 and LS72. They were synthesized at atmospheric pressure by heating mixtures of iron and titanium oxides at 1100°C for 93 h (LS57) and 1300°C for 20 h (LS72) under controlled oxygen fugacity conditions (with CO/CO2 gas mixtures). Products are polycrystalline mixtures of titanomagnetite and ilmenite (modal proportions available in supplementary material), with titanomagnetite grain size in the 50-100 µm range, i.e. large multidomain. Indeed hysteresis measurements up to 1 Tesla (measured using a Micromag VSM) reveal a Mrs/Ms ratio of 0.02 (0.06 for LS57) with remanent coercivity (Bcr) of 2 mT. To increase remanence intensity and stability we finely powdered the samples in an agate mortar and dispersed the powder into epoxy resin. Hysteresis measurements show pseudo-single domain characteristics of the processed samples (suppl. Table S1). Published Curie point values were obtained using magnetic susceptibility versus temperature measurements. The titanium substitution ratii (x=0.73 for LS72 and x=0.74 for LS57) have been determined from electron microprobe analyses of 10 single grains of titanomagnetite in each sample. As the samples were saturated in a 1 T field during VSM measurement, triaxial alternating field demagnetization at 120 mT was applied using the 2G Enterprises DC SQUID Magnetometer prior to the pressure experiment.

Our experimental setup consists of an amagnetic high-pressure cell of piston-cylinder type capable of transmitting hydrostatic pressure to the sample. Our pressure cell is similar to the cell described in [*Sadykov, et al., 2008*] but is entirely made of "russian alloy" (NiCrAl) and has an inner diameter of 8 mm allowing maximum calibrated pressure of 2GPa.The cell is designated specifically to enter into the bore of 2G inline system used for our remanence measurements. Inside the cell itself, the sample is contained in a teflon capsule filled with inert pollyethilsoloxane (PES-1) liquid. The actual pressure at room temperature is about 10% less than the pressure estimated from the known external load [*Sadykov, et al., 2008*].

For each sample, the following protocol was applied: the sample was placed in the cell under a pressure P, then given a uniaxial thermoremanent magnetization along the Z axis. For this, the couple cell-sample was heated at 100°C and placed inside a coil for cooling, under a 751 μT uniaxial field, until it reached RT (20°C). Then a series of thermal demagnetization steps was applied, from 20 to 80°C by steps of 5°C, and from 80 to 110°C by steps of 10°C. After each step, the sample was cooled in a magnetically shielded room at RT and the remanent magnetization **(**RM**)** was measured using the 2G Enterprises DC SQUID Magnetometer. This protocol was iterated for atmospheric pressure, as well as for 300, 600 and 900 MPa.

In order to consider only the TRM acquired by heating to 100°C along Z axis only this component magnetization is plotted. This magnetization is corrected for the residual magnetization measured after reheating in zero field to the maximum temperature. By this way the sample magnetization carried by impurities of higher Curie point (including the residual IRM produced by the hysteresis measurement), as well as the cell magnetization independent of temperature, are removed.

The magnetization of the cell itself was tested prior to the experiment by applying the same protocol to it, and its maximum was found to equal 2% of the weakest initial magnetization. This value was then subtracted to all our data.

3 Correction of the pressure demagnetizing effect

During the heating steps, thermal dilatation of cell components increased the pressure experienced by the sample, and an associated pressure demagnetization was produced [*Bezaeva, et al., 2010*]. This effect had to be estimated and our results corrected from its influence. The initial TRM acquisition also occurs at a higher pressure than the nominal RT one. The pressure change inside the cell was first calculated as a function of applied temperature**,** following the model of *Bezaeva, et al.* [*2015*], using the thermal expansion parameters of the cell and PES-1 liquid:

where is the variation of temperature (in K); and are volume thermal expansion coefficients (in 1/K) of PES-1 and Russian alloy, respectively; is the coefficient of volume compressibility of PES-1; is the sample volume, and is PES-1 volume. ~ $8.5*10^{-4}$ 1/K. for Russian alloy is $33.47*10^{-6}$ 1/K (T=333K), $34.28*10^{-6}$ 1/K (348K), $35.65*10^{-6}$ 1/K (373K), $35.92*10^{-6}$ 1/K (378K) and $36.20*10^{-6}$ 1/K (T=383). These calculated values are in accordance with our experimental data on linear thermal expansion coefficient of Russian alloy for 333K 348K and 373K. values were taken from [*Kagramanyan, 1984*] for suitable P,T conditions (see). ~ /9. Note that this overpressure linked to heating does not apply to the 0 GPa experiment as the piston was not locked allowing dilatation without pressure increase.To estimate the pressure demagnetization of our samples, a series of pressure steps were performed at RT: after acquisition of TRM at atmospheric pressure with the same protocol as described previously, each sample was successively put under constant discrete pressures in the range 0 to 1.4 GPa with steps of 0.2 GPa. Again, after each step, remanent magnetization was measured, using the same setup as before. We were then able to quantify the demagnetizing effect of different pressure values. Finally, we used these results and added them to our data, to access the remanent magnetization corrected from pressure-induced demagnetization (

4 Results

The pressure demagnetization experiments show a TRM decrease to about 55 % of the initial magnetization at P=200MPa, for both samples (). For P between 400 and 1600 MPa, the curves reach a plateau with TRM values between 50 and 40% for LS57, and between 45 and 30% for LS72.

Results of thermal demagnetization for the samples under various pressures are shown in . The LS57 sample appears to produce a less stable signal, likely due to lower Curie point and lower magnetization caused by the smaller titanomagnetite content in the sample.

At ambient pressure the unblocking temperature spectra of the TRM acquired at 100°C can usually be used to estimate a Curie temperature, at the sharpest drop of remanence. For LS57 the corresponding temperature is between 45 and 55 °C, while for LS72 we observe a continuous drop between 55 and 100°C. This is significantly higher than the Tc estimated from susceptibility measurements. Such discrepancy is typical of titanomagnetite according to our experience on basalts. shows that the Curie temperature increases with pressure as shown by a progressive shift of the unblocking temperature. In the case of LS72, it is clear that the unblocking temperature is close to 100°C. The

shift can be roughly estimated to 10-20 K/GPa, in the range previously reported: 10 K/GPa for x= 0.75 [*Schult, 1970*]. This is lower than the reported values for pure magnetite 18 to 23 K/GPa *[Samara and Giardini, 1969; Schult, 1970]*

For the LS72 sample, this increase is correlated with a steepening of the slope of the demagnetization curves: between 337, 675, and 1012 MPa the starting point of the main magnetization decrease shifts from 55-60°C to respectively 90°C and 100°C, and the demagnetization slope from 1.35*10-5 $Am^2.°C^{-1}$ to 4 *10-5 $Am^2.°C^{-1}$.

). This correction is based on the assumption that pressure decrease or increase produce equal demagnetization, as suggested by *Gilder et al* [*2006*]. To precise this critical assumption, this means that pressurizing TRM acquired at 0 MPa from 0 to 200 MPa at RT has the same effect as depressurizing TRM acquired at 1000 MPa from 1000 MPa to 800 MPa at variable temperature from Curie point to RT. This is qualitatively suggested by Fig.2 of *Gilder et al. [2006]* at RT for SD magnetite. However, the analysis of their data table indicates for the 3d compression (from 0.16 GPa) a 16% demagnetization after a first 0.69 GPa increment, while the two decompressions from 2.1 GPa generate a 10 (8)% for a .63 (.65) GPa first decrement. We did not consider the first compression data as the sample obviously suffered irreversible changes in the initial steps. These limited data may suggest that the decompression does not produce equal demagnetization than compression, but only half of it, at RT. On the other hand the fact that in our case decompression occurs just below Curie point, i.e. with a remanent coercivity lower than at RT, should enhance demagnetization efficiency at it increases for decreasing coercivity (Bezaeva et al., 2010). Therefore we propose two possible corrections: one with the equal effect of decompression and compression, and one with a twice smaller effect.

The range of temperatures at which our study took place was limited to values inferior to 110°C in order to avoid too high pressure increase which the cell could not withstand.

4 Results

The pressure demagnetization experiments show a TRM decrease to about 55 % of the initial magnetization at P=200MPa, for both samples (). For P between 400 and 1600 MPa, the curves reach a plateau with TRM values between 50 and 40% for LS57, and between 45 and 30% for LS72.

Results of thermal demagnetization for the samples under various pressures are shown in . The LS57 sample appears to produce a less stable signal, likely due to lower Curie point and lower magnetization caused by the smaller titanomagnetite content in the sample.

At ambient pressure the unblocking temperature spectra of the TRM acquired at 100°C can usually be used to estimate a Curie temperature, at the sharpest drop of remanence. For LS57 the corresponding temperature is between 45 and 55 °C, while for LS72 we observe a continuous drop between 55 and 100°C. This is significantly higher than the Tc estimated from susceptibility measurements. Such discrepancy is typical of titanomagnetite according to our experience on basalts. shows that the Curie temperature increases with pressure as shown by a progressive shift of the unblocking temperature. In the case of LS72, it is clear that the unblocking temperature is close to 100°C. The shift can be roughly estimated to 10-20 K/GPa, in the range previously reported: 10 K/GPa for x= 0.75 [*Schult, 1970*]. This is lower than the reported values for pure magnetite 18 to 23 K/GPa *[Samara and Giardini, 1969; Schult, 1970]*

For the LS72 sample, this increase is correlated with a steepening of the slope of the demagnetization curves: between 337, 675, and 1012 MPa the starting point of the main magnetization decrease shifts from 55-60°C to respectively 90°C and 100°C, and the demagnetization slope from 1.35*10-5 $Am^2.°C^{-1}$ to 4 *10-5 $Am^2.°C^{-1}$.

For both samples we observe variations of TRM intensity at RT as a function of applied pressure (). Uncorrected values increases up to 675 MPa for LS57 and in between 337 and 675 MPa for LS72. These increases are more pronounced after correction with a pressure-related increase of acquired TRM of 50-100% (depending on sample and correction option). For both samples, we also observe a decrease of TRM above 675 GPa.

5 Discussion

The TRM decrease at 1GPa for LS72 could be partially explained by the fact that, due to the limitations of our cell, the TRM of our samples is acquired at a maximum temperature of 110°C. It is possible that the Curie temperature, increasing with pressure, exceeded 110°C at 1 GPa, thus preventing our sample from recording the full TRM spectra compared to lower pressure experiments. Similar experiments at higher temperatures would be needed to validate this hypothesis. Nevertheless, since LS57 Curie temperature is lower than 100°C, the same phenomenon cannot explain the 1GPa RT magnetization decrease for this sample. This suggests that several combined processes may lead to the RT remanent magnetization variations under pressure. The angle of atomic bonds within the crystal structure should not be impacted by hydrostatic pressure [*Gilder, et al., 2004*], but the change in the demagnetizing

slope could indicate the sample evolved toward a more single domain-like state. However, these results need to be reproduced with other types of samples in order to calibrate the influence of the nature of the sample on the experiment.

Nevertheless, the Curie isotherm depth is usually calculated using reasonable estimations of the (potentially stable) thermal gradient of the crust/lithosphere and/or by processing the magnetic field anomaly data [*Mayhew, 1982; Blakely, et al., 1986; Bouligand, et al., 2009*], considering magnetite as the main carrier of the crustal/lithospheric magnetism [*Langel, et al., 1998*]. The 10°C shift in Tc revealed by our pressure experiments would then imply a shift of the Curie depth up to a value of 6%, depending on the thermal gradient.

For instance, the Curie isotherm can be as shallow as <1 km in some volcanic areas, as well as more than 60 km deep in the lithosphere under cratonic regions [*Negi, et al., 1987*]. This implies the same variability for the importance of the modification that should be applied: in the regions with high thermal gradient, where the isotherm is shallow, the shift would only be of less than 100m. On the contrary, in low thermal gradient areas, the difference could reach 3 to 4 kilometers. Furthermore, since TRM acquired under pressure may be stronger than TRM acquired at atmospheric pressure, then a large part of the lithosphere magnetism could be underestimated. Our work shows a significant increase starting between 337 and 675 MPa (depending on the main magnetic mineral), this implies that rocks located below a depth limit oscillating between 13 and 20 km could have a magnetization two times higher than what is currently admitted.

This change could have an important impact on magnetic crustal models using deep sources, especially since most of the biggest magnetic anomalies on Earth are located inside cratons [*Ravat, et al., 1991; Langel, et al., 1998; Ouabego, et al., 2013*], where the corrected Curie depth has a chance to be the most different from the current one, and where the potentially overmagnetized part of lithosphere is the thickest. Stronger magnetization at large depths could also mean smaller sources in some models.

One has to keep in mind that without remanence, the magnetic layer necessary to explain the large magnetic field anomalies reaches too large depths [*Vervelidou, et al., 2015*]. *Usui, et al.* [*2015*] have also shown that lamellae exsolution may produce strong remanence at middle to lower crust depths, at least for granulite rocks exposed in cratonic regions. *McEnroe et al.* [*2004*] conducted pressure experiments on such granulite rocks and showed that hematite-ilmenite exsolutions are also good candidates to carry this magnetism. Not only the current P-T conditions and magnetic mineralogy influence the magnetism of crustal layers, but also their metamorphic degree [*Wang et al., 2015*], including low-T alterations. Nevertheless, many recent studies have shown that the magnetic layer may reach the mantle itself [*Ferré et al., 2013; Li et al., 2015*], which correlates to our results. Finally, such experimental studies have implications for other remanently-magnetized planetary lithospheres, like on Mars and the Moon, since most source models suggested large depths as the origin of the largest magnetic field anomalies [*Quesnel et al., 2007; Langlais et al., 2004; Takahashi et al., 2014*].

6 Conclusion

The hydrostatic pressure experiments conducted with a liquid confining media pressure cell up to 1012 MPa show that TRM acquisition and demagnetization of titanomagnetite is susceptible to pressure change. At higher pressures, the Curie temperature increases up to a measured maximum of +10°C at 1012MPa for both minerals compared to atmospheric pressure. The hydrostatic pressure applied allows us to free ourselves from the deviatoric strain, and make this experiment as close as possible to in situ deep crustal conditions. These results support the idea that pressure has to be taken into account when dealing with the crust magnetization, and especially when working with Curie isotherms. A correction of the currently admitted Curie depth might have to be considered, mostly for low thermal gradient cratonic regions, where it could be 3 to 4 km deeper than previously thought. In addition to that, we showed that the TRM acquired under pressure can be twice as strong as the one acquired under atmospheric conditions. Assuming that our results on Ti rich titanomagnetite can be extrapolated to nearly pure magnetite**,** these results suggest a new perspective about the sources of Earth magnetic anomalies.

Acknowledgments

Supporting data are included as three figures and one table in the supporting information; any additional data may be obtained from N.L. (email: launay@cerege.fr). Work is supported by Act 211 Government of the Russian Federation, agreement No. 02.A03.21.0006 and is performed according to the Russian Government Program of Competitive Growth of Kazan Federal University. J. Gattacceca is thanked for his help on the pressure cell.

References

Bezaeva, Natalia S, et al. 2010. Demagnetization of terrestrial and extraterrestrial rocks under hydrostatic pressure up to 1.2GPa. Physics of the Earth and planetary interiors. 2010, Vol. 179, pp. 7-20

Bezaeva, Natalia S, et al. 2007. Pressure demagnetization of the Martian crust: Ground truth from SNC Meteorites. Geophysical Research Letters. 2007, Vol. 34.

Bezaeva, Natalia S, et al. 2015. The effect of hydrostatic pressure up to 1,61GPa on the morin transition of hematite bearing rocks: implications for planetary crustal magnetization. Geophysical Research Letters. 2015, Vol. 42.

Blakely, Richard J. et Simpson, Robert W. 1986. Approximating edges of source bodies from magnetic or gravity anomalies. Geophysics. 1986, Vol. 51, pp. 1494-1498.

Bouligand, Claire, Glen, Jonathan M.G et Blakely, Richard J. 2009. Mapping Curie temperature depth in the western United States with a fractal model for crustal magnetization. Journal of Geophysical Research. 2009, Vol. 114.

Demory, F, et al. 2013. Remanent magnetization and coercivity of rocks under hydrostatic pressure up to 1.4GPa. Geophysical Research Letters. 2013, Vol. 40, pp. 3858-3862.

Dunlop, David J. et Özdemir, Özden. 1997. Rock Magnetism: fundamentals and frontiers. 1997.

Engelmann, Ralf, Kontny, Agnes et Lattard, Dominique. 2010. Low temperature magnetism of synthetic Fe-Ti oxide assemblages. Journal of Geophysical Research. 2010, Vol. 115.

Ferré, Eric C., et al. 2013. The magnetism of mantle xenoliths and potential implications for sub-Moho magnetic sources. Geophysical Research Letters. 2013, Vol. 40.

Ferré, Eric C., et al. 2014. Eight good reasons why the uppermost mantle could be magnetic. Tectonophysics. 2014, Vol. 624-625, pp. 3-14.

Friedman, S.A., et al. 2014. Craton vs. rift uppermost mantle contributions to magnetic anomalies in the United States interior. Tectonophysics. 2014, Vol. 624-625, pp. 15-23.

Gilder, S. et Le Goff, M. 2008. Systematic pressure enhancement of titanomagnetite magnetization. Geophysical Research Letters. 2008, Vol. 35.

277 Gilder, S., et al. 2004. Magnetic properties of single and multi-domain
278 magnetite under pressure from 0 to 6 GPa. Geophysical Research Letters. 2004,
279 Vol. 31.

280 Gilder, Stuart A., Le Goff, Maxime et Chervin, Jean-Claude. 2006. Static stress
281 demagnetization of single and multidomain magnetite with implications for
282 meteorite impacts. High Pressure Research. 2006, Vol. 26.

283 Kagramanyan, L. S. (1984), Elastic and thermodynamic properties of a series of
284 silicone fluids at pressures of up to 600 MPa from acoustic measurements, PhD
285 thesis, Yerevan Polytech. Inst., Yerevan.

286 Langel, R. A. et Hinze, W. J. 1998. The magnetic field of the Earth's lithosphere.
287 1998.

288 Langlais, B., Purucker, M. et Mandea, M. 2013. Crustal magnetic field of Mars.
289 Journal of Geophysical Research. 2013.

290 Li, Zhiyong, et al. 2015. Magnetically stratified continental lower crust
291 preserved in the North China Craton. Tectonophysics. 2015, Vol. 643, pp. 73-79.

292 Mayhew, M.A. 1982. Application of Sattelite magnetic anomaly data to curie
293 isotherm mapping. Journal of Geophysical Research. 1982, Vol. 87, pp. 4846-4854.

294 McEnroe, S.A., et al. 2004. What is magnetic in the lower crust? Earth and
295 Planetary Science Letters. 2004, Vol. 226, pp. 175-192.

296 Negi, J. G., Agrawal, P. K. et Pandey, O. P. 1987. Large variation of Curie depth
297 and lithospheric thickness beneath the indian subcontinent and a case for
298 magnetothermometry. Geophysical Journal Royal Astronomical Society. 1987,
299 Vol. 88.

300 Ouabego, M., et al. 2013. Rock magnetic investigation of possible sources of the
301 Bangui magnetic anomaly. Physics of the Earth and Planetary interiors. 2013,
302 Vol. 224, pp. 11-20.

303 Pearce, G W et Karson, J A. 1981. On pressure demagnetization. Geophysical
304 Research Letters. 1981, Vol. 8, pp. 725-728.

305 Pozzi, J.P. 1975. Magnetic properties of oceanic basalts - Effect of pressure and
306 consequences for the interpretation of anomalies. Earth and Planetary
307 Science Letters. 1975, Vol. 26, pp. 337-344.

308 Quesnel, Y., et al. 2007. Local inversion of magnetic anomalies: Implication for
309 Mars' crustal evolution. Planetary and Space science. 2007, Vol. 55, pp. 258-269.

310 Ravat, D. N., Hinze, W. J. et von Frese, R.R.B. 1991. Analysis of MAGSAT
311 magnetic contrasts across Africa and South America. Tectonophysics. 1991,
312 Vol. 212, pp. 59-76.

Sadykov, Ravil A, et al. 2008. Nonmagnetic high pressure cell for magnetic remanence measurements up to 1.5GPa in a superconducting quantum interference device magnetometer. Review of Scientific instruments. 2008, Vol. 79.

Samara, G.A., et Giardini, A.A. 1969. Effect of ressure on the Néel temperature of magnetite. Physical Review. 1969, Vol. 186, pp. 577-580.

Schult, A. 1970. Effect of pressure on the Curie temperature of titanomagnetites (1-x) Fe3O4xFe2TiO4. Earth and Planetary Science Letters. 1970, Vol. 10, pp. 81-86.

Takahashi, Futoshi, et al. 2014. Reorientation of the early lunar pole. Nature Geoscience. 2014.

Thébault, Erwan, et al. 2016. A SWARM mithospheric magnetic field model to SH degree 80. Earth, Planet and Space. 2016.

Usui, Yoichi, et al. 2015. Rock magnetism of tiny exsolved magnetite in plagioclase from a paleoarchean granitoid in the pilbara craton. Geochemistry, Geophysics, Geosystems. 2015, Vol. 16, pp. 112-125.

Vervelidou, F. et Thébault, E. 2015. Global maps of the magnetic thickness and magnetization of the Earth's lithosphere. Earth Planets and Space. 2015, Vol. 67.

Wang, Hongcai, et al. 2015. Magnetic properties of Archean gneisses from the Northeastern North China Craton: the relationship between magnetism and metamorphic grade in the deep continental crust. Geophysical Journal International. 2015, Vol. 201, pp. 475-484.

Table 1: Various values used to correct raw data from the impact of pressure demagnetization. Pi = initial pressure applied; Tc = Curie temperature; Pr = effective pressure at Tc; ΔP = Pr – Pi; ΔTRM = TRM variation caused by pressure change ΔP . The two options discussed in §2.1 for TRM correction are reported with the lower correction in brackets.

Sample	**Pi** (MPa)	**Tc** (°C)	**Pr** (MPa)	**ΔP** (MPa)	**ΔTRM** (% initial TRM)	**measured TRM** (μAm^2)	**corrected TRM** (μAm^2)
LS72	*0.1*	*100*	*0.1*	*0*	*0.0*	*10.0*	*10.00*
	337	*100*	*581*	*244*	*-47.3 [-23.7]*	*4.29*	*8.15 [5.62*
	675	*105*	*1084*	*409*	*-57.5*	*8.40*	*19.7 [11.8]*
	1012	*110*	*1445*	*433*	*-58.3*	*6.05*	*14.5 [8.54]*
LS57	*0.1*	*55*	*0.1*	*0*	*0.0*	*1.01*	*1.01*
	337	*60*	*465*	*128*	*-31.5*	*1.10*	*1.61 [1.31]*
	675	*60*	*875*	*200*	*-40.6*	*1.10*	*1.86 [1.39]*
	1012	*75*	*1281*	*269*	*-46.2*	*0.745*	*1.39 [0.969]*

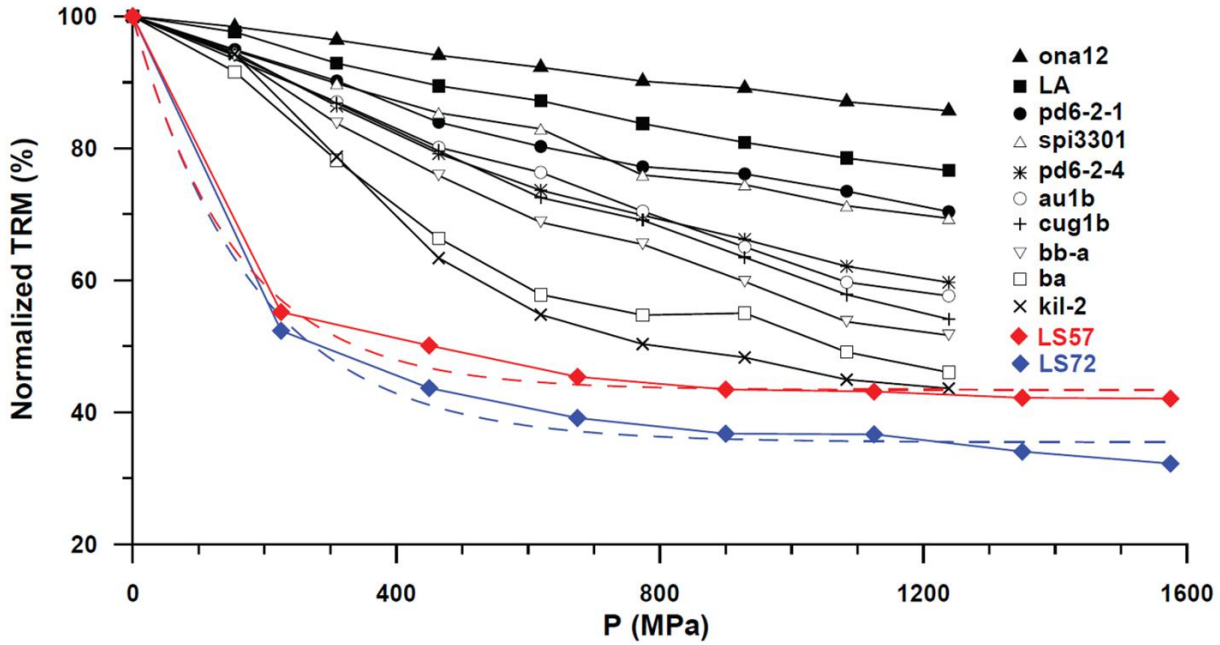

*Figure 1: Normalized TRM as a function of applied pressure (P) at room temperature. It is important to note that our data are presented along the data obtained for SIRM pressure demagnetization experiments on titanomagnetites by [Bezaeva, et al., 2010]. For our data, the solid lines represent measured values, while the dotted lines represent the best-fit trend curves. The trend curves equations are, for LS57 and LS72 respectively: y=56.4*exp(-0.0063*x)+43.4 and y=64.25*exp(-0.0054*x)+35.43*

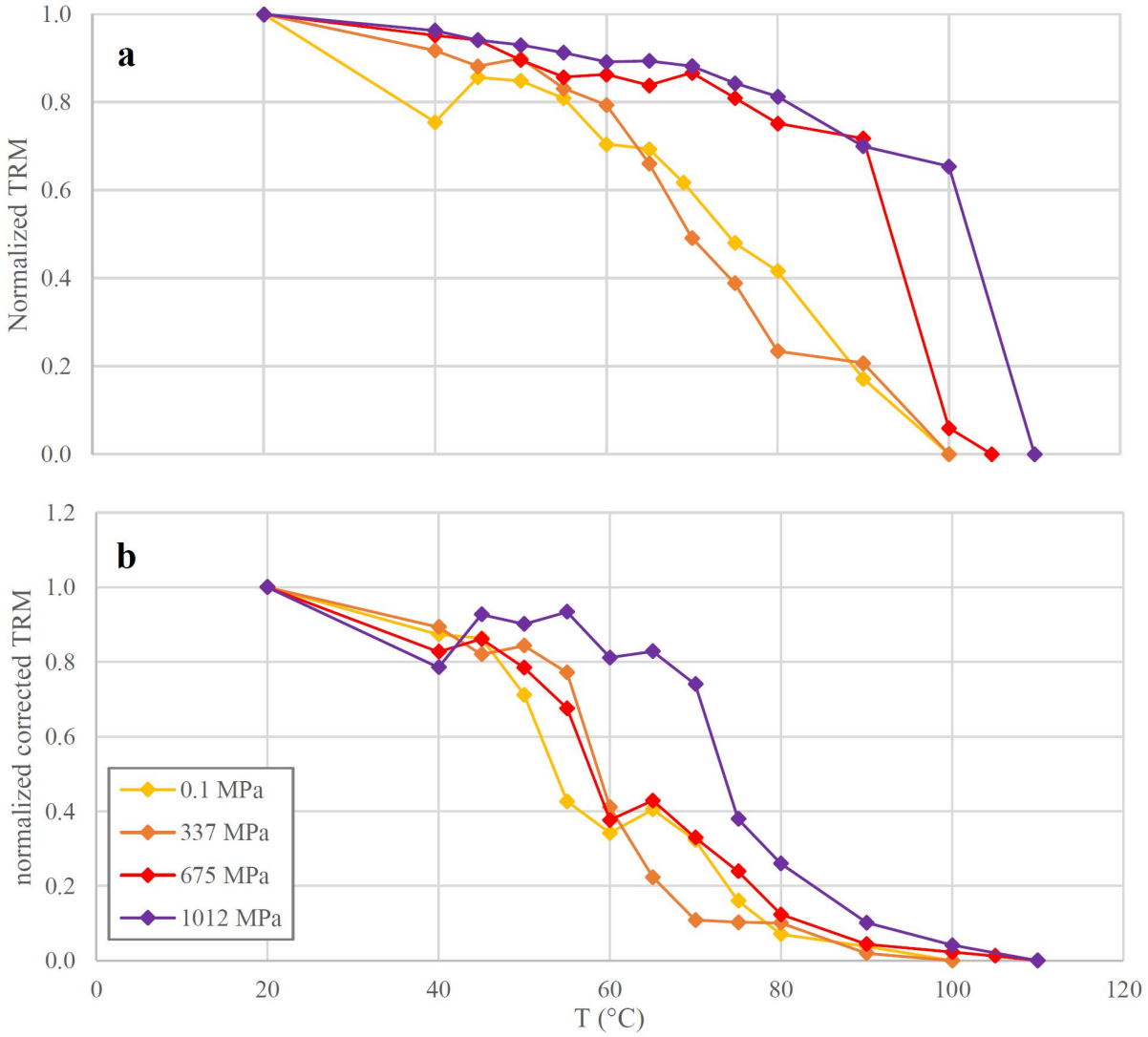

345

346 *Figure 2: Normalized Z intensity of TRM for both samples as a function of demagnetization temperature, for different pressures.*
347 *(a)LS72 values. (b) LS57 values. Indicated pressure values correspond to Pi (see Table 1).*

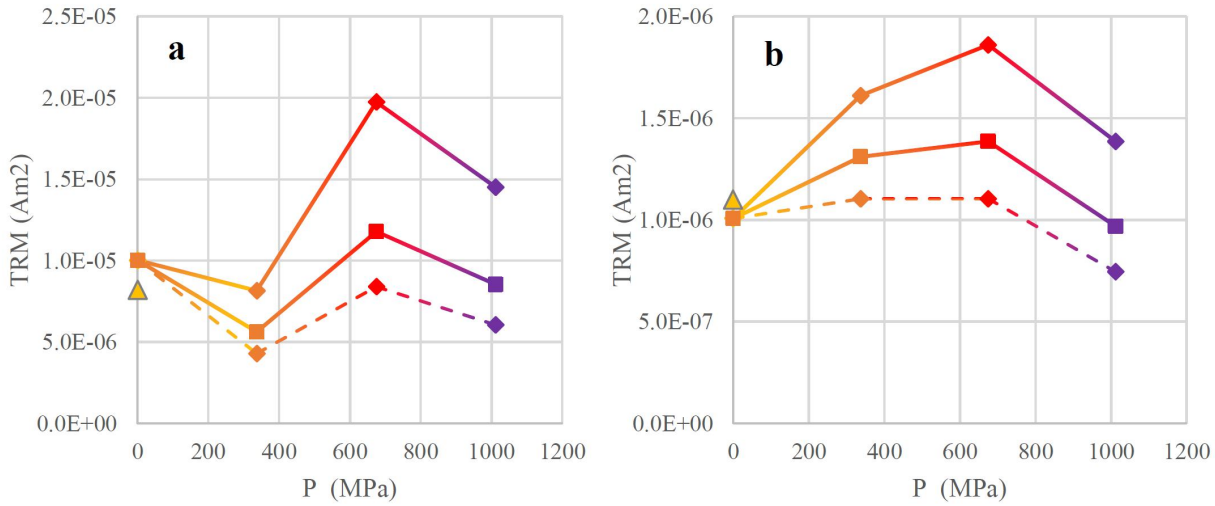

Figure 3: TRM at room temperature (RT) as a function of applied pressure for LS72 (a) and LS57 (b). Dotted lines represent the measured values, and solid lines represent the corrected values in the two hypothesis discussed in § 2.1(squares = lower correction). The outlined triangles represent TRM acquired under atmospheric pressure after decompression from 1 GPa.